Fibers and Polymers 2012, Vol.13, No.7, 874-879 DOI 10.1007/s12221-012-0874-5

Carbon Nanotube/Poly(vinyl alcohol) Fibers with a Sheath-core Structure Prepared by Wet Spinning

Giryong Park, Yeonsu Jung, Geon-Woong Lee[1], Juan P. Hinestroza[2], and Youngjin Jeong*

Department of Organic Materials and Fiber Engineering, Soongsil University, Seoul 156-743, Korea
[1]Nano Carbon Materials Research Group, Korea Electrotechnology Research Institute (KERI)
[2]Department of Fiber Science & Apparel Design, Cornell University, NY, USA
(Received January 2, 2012; Revised February 3, 2012; Accepted February 11, 2012)

Abstract: A method for manufacturing sheath-core structured fibers was developed using wet spinning techniques. The core portion of a fiber was prepared using a carbon nanotube (CNT) solution while the sheath used a fiber-forming polymer such as polyvinyl alcohol (PVA). Preparation methods of CNT solutions were investigated and it was found that dispersivity and concentration played an important role in the formation and spinning of fiber's core. CNT solution prepared using a surfactant with high molecular weight such as sodium lignosulfonate (SLS) was most effective and the CNT concentration was as high as 30 g/*l*. Fiber processing conditions were optimized and it was determined that stretching fibers in the coagulation bath was a significant step in the formation of a solid and well structured core. Drawn fibers were so strong and flexible that they could be woven into a fabric for potential use as a pressure sensor. These results are relevant for practical applications, such as the development of large-area fabric sensors. Furthermore, the described procedure to produce sheath-core CNT fibers is scalable as wet spinning methods have been widely used in the fiber industry.

Keywords: Carbon nanotube, Fiber, Sheath-core, Wet spinning, Dispersion

Introduction

Carbon nanotubes (CNTs) have a high tensile strength, low mass density, high heat conductivity, and high electrical conductivity [1]. The outstanding properties of CNTs and their unique 1D nanostructure allow for a wide range of potential applications, such as structural fibers, composites, and multifunctional fabrics [2-6]. CNT/polymer composite fibers have attracted much interest due to the unique properties of CNTs however, the use of CNTs as a filler has been limited due to issues regarding their dispersion stability and their interfacial interactions mediated by van der Waals forces. Several processes have been developed for weaving CNTs into continuous CNT fibers, which is an essential step toward the development macroscopic applications. Representative processes include injection of surfactant-dispersed nanotubes into a rotating beaker containing aqueous polyvinyl alcohol [7,8], liquid crystalline spinning of an acid dispersion [9], dry spinning from aligned CNT arrays grown on a substrate [10,11], and direct spinning through a chemical vapor deposition (CVD) [12]. CNT fibers with appropriate physical and mechanical strength are required for the fabrication of 2D assemblies such as fabrics so these assemblies could be used as catalyst supports [14], filtration systems [15], conductors [16], electromagnetic shields [17], capacitors [13], and large-area pressure sensors.

In this manuscript, we report a new method for manufacturing CNT fibers with sheath-core structures via wet spinning. Figure 1 shows a schematic diagram of the approach pursued in this study. The sheath-core structure is produced by using a double nozzle of which the core is filled with a high-concentration CNT solution, and the sheath segment is filled with a fiber forming polymer solution such as polyvinyl alcohol (PVA). Other polymers may be used, depending on the final application of the sheath-core CNT fibers. The described spinning method offers extensive possibilities for tuning the mechanical and physical properties of CNT fibers. For example, the mechanical and physical properties of fiber can be modulated by controlling the gap distance between the nozzle tip and the coagulation solvent as the most molecular orientation occurs in that region. The solvent composition of the coagulation bath is also important because of potential cross-diffusion issues with the fiber forming polymer solution used for the sheath.

We aimed our work at determining the proper conditions that would allow the continuous spinning of sheath-core structured fibers. PVA was selected as a sheath polymer as

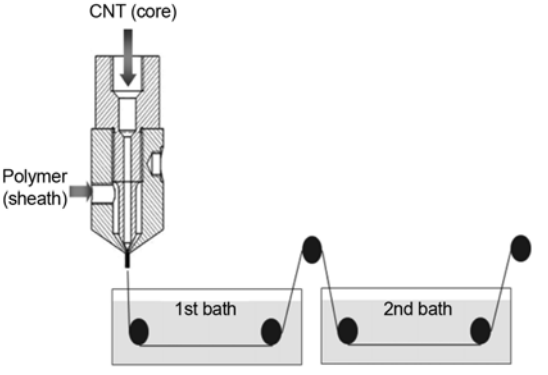

Figure 1. The wet spinning process used to produce the sheath-core structured CNT/PVA fiber.

*Corresponding author: yjeong@ssu.ac.kr

there are several reports of its previous use in CNT coagulation spinning processes [7,18]. The preparation on CNT solutions is also an area of focus because aggregated CNT solutions tend to clog the nozzle and prevent CNTs from forming a continuous fiber. The drawing effects were also examined as the stretching ratio is known to be a critical factor in determining the mechanical properties of the fibers.

Experimental

Materials

Multiwalled carbon nanotubes (MWNTs) with a purity of 95 wt%, a diameter of 20-40 nm, and lengths of 5-20 μm were produced via chemical vapor deposition (CVD) and supplied by JEIO technologies (Korea). Sodium lignosulfonate (SLS), with an average molecular weight of 52,000, was purchased from Sigma Aldrich as used as the dispersion surfactant. PVA was supplied by Tex-tech in Korea. The degree of polymerization and saponification of the PVA was reported to be 1,700 and 99 % respectively. Dimethyl sulfoxide (DMSO) with a 99 % purity was purchased from Samchun Chemical (Korea) and used to prepare the PVA solutions. Methanol with a purity of 99.5 % was purchased from Samchun Chemical (Korea) and used as the coagulation bath.

Preparation of Dope Solutions

Separate dope solutions were prepared for the core and sheath of the composite fiber. The core portion of the fiber was composed of an aqueous CNT solution prepared in either one of the following two procedures: acid functionalization of MWNTs or surfactant treatment using sodium lignosulfonate (SLS). For acid functionalization, MWCNTs were ultrasonicated in a mixture of sulfuric acid and nitric acid (3:1) for 2 h using a Sonics & Materials Inc. bath sonicator (20 kHz, 150 W). The mixture was then stirred at 90 ^{o}C under reflux for 2 h. The solution was cooled to room temperature and diluted several times with deionized water until the pH was approximately 7. The solution was then filtered using 8-μm pore cellulose filter paper and dried for one week in a freeze drier. MWNT functionalization via surfactants was accomplished by adding SLS in an agate mortar and grinding the solution for 10 min by hand with the addition of a small quantity of water to avoid agglomeration. The ground mixture was diluted with distilled water and sonicated for 10 min. The dope solution for the sheath segment was prepared by dissolving PVA (13 wt%) in DMSO at 90 ^{o}C and allowing the solution to sit for one day at ambient conditions to remove air bubbles trapped.

Spinning of Sheath-core Structured Fibers

Figure 1 illustrates the wet process set-up used to spin sheath-core structured CNT fibers. The system consisted of a double nozzle of inner and outer holes. The holes were connected to separate syringe pumps that were independently driven to control the flow rates of the two solutions. The CNT solution was injected into the inner nozzle and the PVA polymer solution to the outer nozzle. The inner and outer diameters of the spinneret were 0.3 mm and 0.5 mm. The air gap between spinneret and coagulation bath was set to 3 cm. The fibers were spun using several concentrations of CNT solution and varying speeds of the rollers in the 2nd coagulation bath to impart various stretching ratios to the fiber. The discharge pressures of the core and sheath, for all samples, were 6 kPa and 200 kPa.

Characterization

The dispersability of the MWNT solutions was verified via optical microscopy (Sometech, IMS-D-345). The morphologies of the spun fibers were characterized using field emission scanning electron microscopy (FE-SEM, FEI-Sirion 400 (JSM 6500F)). A universal test machine (Instron 4464) was used to measure the tensile properties of the spun fibers and a digital multimeter (Fluke, 87III) was used to perform electrical conductivity measurements.

Results and Discussion

The use of a highly concentrated and well-dispersed CNT solutions was found to be a critical factor for proper injecting of the dope through the spinning nozzle as aggregated CNTs easily clogged the spinning nozzle and low-concentration CNT solutions failed to form continuous core fibers.

Preparation of Fibers by Acid-functionalized MWNTs

Acid-functionalized MWNT solutions of different concentrations were evaluated. The maximum concentration of aqueous CNT solution achieved via acid treatment was 10 g/*l*; however this concentration of CNT was not sufficient to fill the core of a fiber. To prepare CNT solutions with higher concentrations, the solution pH was adjusted using NaOH as COOH deprotonation on the CNT surfaces has been reported to increase with pH [19]. Deprotonation of COOH groups forms H^{+} cations and -COO^{-} anions hence inducing the CNTs to repel one another. This repulsion induces the loosening CNTs bundles yielding individual well-dispersed CNTs. By adjusting pH value to pH 10 a concentration as high as 50 g/*l* was achieved. Allowing the solution to settle for one day removed aggregated CNTs via precipitation. After removal of the decanted aggregates the resulting CNT solution (30 g/*l*) was used in the spinning process and the nozzle was no longer clogged. Cross-sections of fibers spun using acid-functionalized CNTs at two concentration levels are shown in Figure 2. It can be observed that most of the fiber cross-sections were not filled with CNTs and this anomaly can be attributed to the presence of water in the CNT solution which probably effused out of the sheath polymer during fiber formation. Voids in the fiber could be

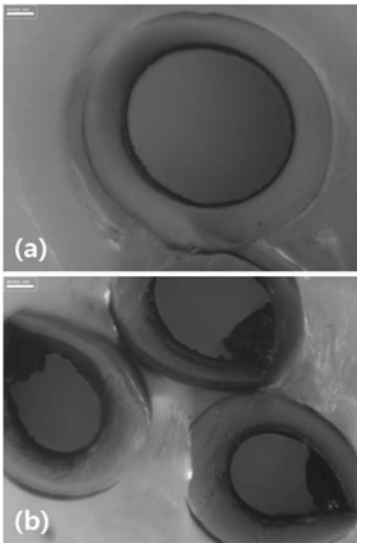

Figure 2. Optical microscopy images of MWNT fiber cross-sections (×1000) spun from 10 g/*l* (a), 30 g/*l* (b) MWNT solutions for the core, and PVA for the sheath.

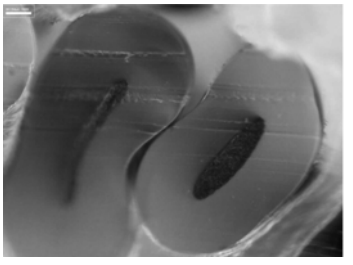

Figure 3. An optical image (×1000) showing the drawing effect on the cores of fibers made from acid-functionalized CNTs (30 g/*l*). The speed of the rollers in the 1st bath was set to 20 m/min and that of the 2nd bath was set to 40 m/min.

reduced by adjusting the roller speed to an optimal fiber drawing speed hence tightening the core segment. The speed of the rollers in the 1st bath was set to 20 m/min whereas the speed of the rollers in the 2nd bath was varied to 20, 40, and 87 m/min giving different stretch ratios to the spun fiber. Figure 3 illustrates that the incorporation of fiber drawing removed the empty spaces within the core but core segment was distorted into an oval shape.

Preparation of Fibers by Surfactant-functionalized MWNTs

SLS was previously investigated as a surfactant for the noncovalent functionalization of CNTs by Liu *et al.* [20]. SLS possesses a hydrophobic backbone consisting of many aromatic rings linked by C3 ethers and a carbon bond. SLS efficiently disperses CNTs in water due to the presence of several surface anionic groups. These properties make SLS useful for dispersing pesticides, dyes, carbon black, or other insoluble solids and liquids in water. It has been reported that CNTs can be functionalized through π-π interactions

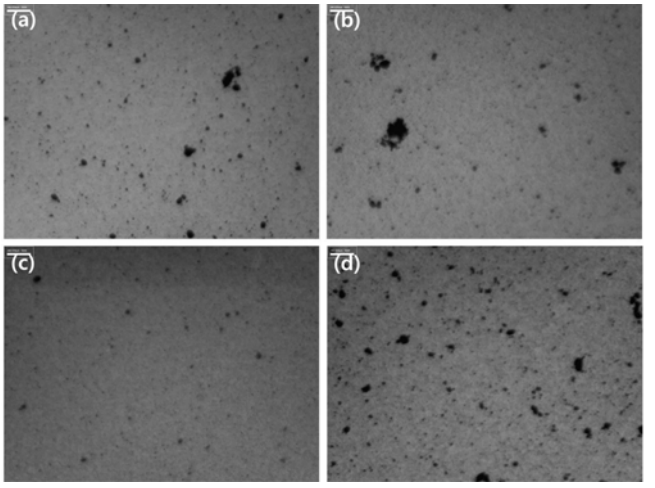

Figure 4. Optical microscopy images of MWNT solutions prepared using SLS (×500). The ratios of MWNTs to surfactant were (a) 1:1, (b) 1:5, (c) 1:10, and (d) 1:15 by weight.

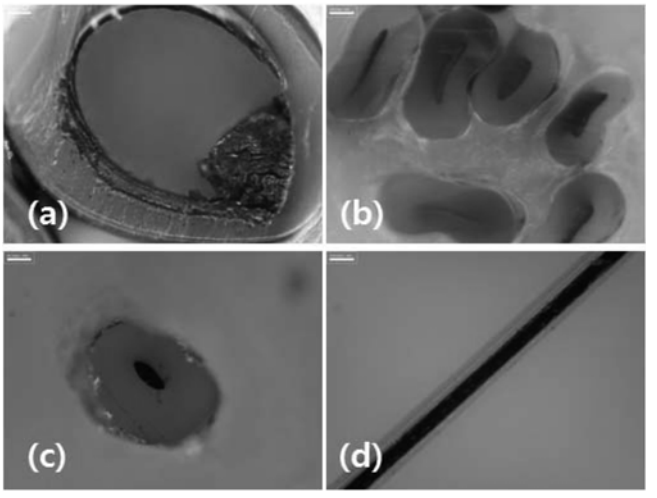

Figure 5. Optical microscopy images of fibers spun at different stretching ratios (a) cross-section of a non-stretched fiber (roller speed; 20 m/min, ×1000), (b) cross-section of a stretched fiber (roller speed: 40 m/min, ×1000), (c) cross-section of a stretched fiber (roller speed: 87 m/min, ×1000), (d) side view of a the previous fiber specimen.

and hydrophobic attraction of the alkyl chains of SLS [20]. The optimum amount of SLS needed to functionalize MWNTs was carefully investigated [21] because excess of SLS can degrade the properties of CNTs by inducing wrapping. In this study, the optimum ratio of SLS to CNT was 10:1, determined via optical microscopy imaging of the solutions as shown in Figure 4. CNT solution concentrations of 30 g/*l* were prepared using a 10:1 SLS:CNT ratio and spun at varying stretching ratios.

Figure 5 shows optical images of fiber cross-sections spun at varying stretching ratios. The fiber spun under zero

Figure 6. Image of a CNT composite fiber spun from a MWNT solution dispersed with SLS in methanol. The brown color indicates the migration of SLS/water through the sheath PVA into the methanol bath.

stretching exhibits many empty spaces within the core whereas the specimens spun at a higher stretching ratio do not. The removal of empty spaces is attributed to the stretching of the fibers while they were immersed in the coagulation bath. During the stretching process, the PVA used in the sheath segment is also drawn and the core segment is tightened by the circumambient PVA. The magnitude of the tightening was proportional to the ratio of the 2nd roller speed to the 1st roller speed (draw ratio), which induced water in the CNT solution to diffuse throughout the polymer into the methanol bath and Figure 6 illustrates this phenomenon. After the spun fibers were placed in methanol for 30 min, the transparent methanol solution turned into a brown color which indicates the presence of SLS. Figure 5(d) shows that oval-shaped stretched fiber specimens with a uniform continuous core filled with CNTs The SLS-dispersed CNT solution appears to form a more uniform continuous core which can be attributed to the presence of minor wrapping of the MWNTs by the SLS.

The sheath-core structured fiber spun from the SLS-dispersed CNT solution and stretched by the 2nd roller at a speed of 87 m/min was further analyzed. Figure 7 shows the cross-section of the fiber illustrating that the sheath and core are firmly contacted at the boundary (Figure 7(a) and 7(b)). The stretching effects are apparent in Figure 7(c), in which many CNT ends are exposed suggesting that CNTs were aligned along the fiber axis. Figure 8 shows the stress-strain curves of neat PVA and CNT/PVA sheath-core fibers. It can be observed that the modulus was not affected by the presence of a sheath-core structure but he breaking strength and elongation were reduced slightly. Small changes in the

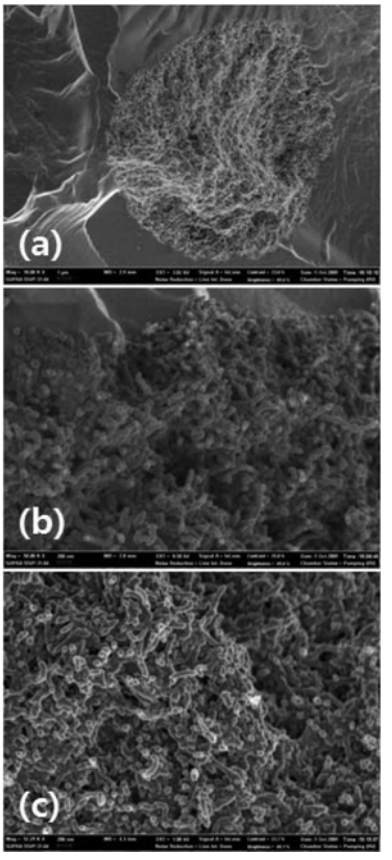

Figure 7. FE-SEM images of a sheath-core structured MWNT fiber spun from a CNT solution dispersed with SLS, (a) ×10,000, (b, c) ×50,000. Image (c) shows many exposed CNT ends suggesting that CNTs were oriented along the fiber.

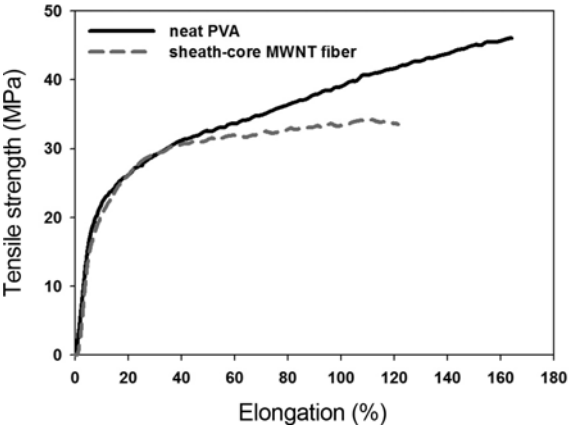

Figure 8. Stress-strain curves of neat PVA fibers and sheath-core MWNT fibers.

modulus imply that contact between the sheath and the core was sufficiently strong to bear the initial deformation, as shown in Figures 7(a) and 7(b).

The electrical conductivity of the composite fiber was

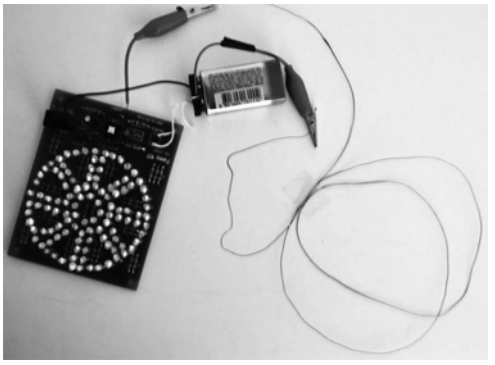

Figure 9. Visual presentation of the conductivity of the fiber prepared using a PVA sheath and a CNT solution dispersed with SLS.

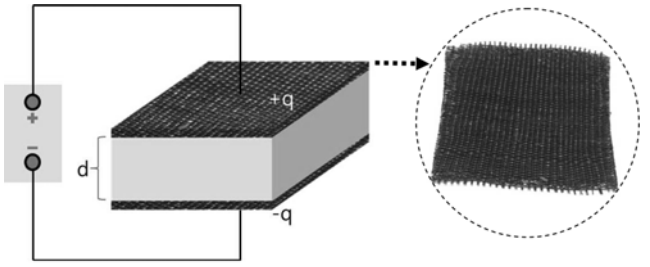

$$C = \varepsilon_0 \varepsilon_r \frac{A}{d}$$

C : the capacitance (F)
ε_0 : the electric constant ($\varepsilon_0 \approx 8.854\times10^{-12}$ F/m)
ε_r : the relative static permittivity (F/m)
A : the area of overlap of the plates (m^2)
d : the separation between the plates (m)

Figure 10. Principles underlying the fabric sensor which responds to changes in the capacitance. The capacitance is inversely proportional to the distance between the conductive fabrics. The inset shows the conductive fabric woven from the sheath-core structured CNT/PVA fibers.

measured using a digital multimeter (Fluke, 87III). The conductivity was determined to be 3.4×10^3 S/m which is sufficiently high to turn on a series of diodes, as shown in Figure 9. The yarn was flexible enough for weaving into a fabric configuration. The inset of Figure 10 shows a woven fabric made from the sheath-core fibers and subsequently used to fabricate a pressure sensor. The fabric sensor responded to pressure by detecting a change in the capacitance, as illustrated in Figure 10. The capacitance depended on the distance between two conductive plates. Here, the fabric woven from the CNT composite fibers was used as the plates and a middle layer was not required because the sheath part of the fiber played this role. Figure 11 shows the response of the fabric sensor to the touch of fingertips, which induced a bulb to flash by sensing changes in the distance between fabrics.

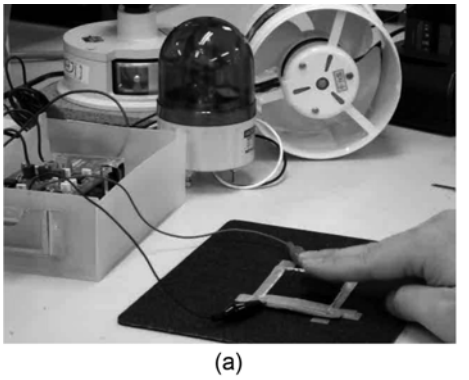

Figure 11. The response of the fabric sensor to the touch of fingertips, (a) before and (b) after touch.

Conclusion

Fibers with a well-defined sheath-core structure, in which CNTs composed the core, were prepared using wet spinning methods. The fibers were formed from highly concentrated and well-dispersed CNT solutions prepared using two different procedures: acid functionalization procedure and surfactant induced dispersion, Dispersion of CNTs using SLS was found to be more effective as SLS induces wrapping the CNTs hence enhancing fiber formation. The interfacial contact between the core and sheath was found to be good and did not hindered flexibility of the resulting fibers so they could be easily woven into a fabric. The spinning technology used here is scalable and offer many possibilities as wet spinning is compatible with mass production methods widely used in industry. A pressure sensor was created to demonstrate the potential use of CNT sheath-core fabrics in the development of smart and interactive textiles.

Acknowledgments

This work was supported by the Fundamental R&D Program for Core Technology of Materials and the Human Resources Development Project of the Korea Institute of Energy Technology Evaluation and Planning (KETEP) (No.0104010100610) in grants funded by the Ministry of

Knowledge Economy, Republic of Korea.

References

1. X. F. Zhang, Q. W. Li, Y. Tu, Y. A. Li, J. Y. Coulter, L. X. Zheng, Y. H. Zhao, Q. X. Jia, D. E. Peterson, and Y. T. Zhu, *Small*, **3**, 244 (2007).
2. W. A. de Heer, A. Chatelain, and D. Ugarte, *Science*, **270**, 1179 (1995).
3. C. J. Lee, J. Park, S. Y. Kang, and J. H. Lee, *Chem. Phys. Lett.*, **326**, 175 (2000).
4. Y. Nakayama and S. Akita, *Synth. Met.*, **117**, 207 (2001).
5. W. I. Milne, K. B. K. Teo, G. A. J. Amaratunga, P. Legagneux, L. Gangloff, J. P. Schnell, V. Senmet, V. T. Binh, and O. Groening, *J. Mater. Chem.*, **14**, 933 (2004).
6. P. Calvert, *Nature*, **399**, 210 (1999).
7. B. Vigolo, A. Pénicaud, C. Coulon, C. Sauder, R. Pailler, C. Journet, P. Bernier, and P. Poulin, *Science*, **290**, 1331 (2000).
8. B. Dalton, S. Collins, E. Munoz, J. M. Razal, V. H. Ebron, J. P. Ferraris, J. N. Coleman, B. G. Kim, and R. H. Baughman, *Nature*, **423**, 703 (2003).
9. L. M. Ericson, H. Fan, H. Q. Peng, V. A. Davis, W. Zhou, J. Sulpizio, Y. H. Wang, R. Booker, J. Vavro, C. Guthy, A. N. G. Parra-Vasquez, M. J. Kim, S. Ramesh, R. K. Saini, C. Kittrell, G. Lavin, H. Schmidt, W. W. Adams, W. E. Billups, M. Pasquali, W. F. Hwang, R. H. Hauge, J. E. Fischer, and R. H. Smalley, *Science*, **305**, 1447 (2004).
10. K. L. Jiang, Q. Q. Li, and S. S. Fan, *Nature*, **419**, 801 (2002).
11. M. Zhang, K. R. Atkinson, and R. H. Baughman, *Science*, **306**, 1358 (2004).
12. Y. L. Li, I. A. Kinloch, and A. H. Windle, *Science*, **304**, 276 (2004).
13. D. N. Futaba, K. Hata, T. Yamada, T. Hiraoka, Y. Hayamizu, Y. Kakudate, O. Tanaike, H. Hatori, M. Yumura, and S. Iijima, *Nat. Mater.*, **5**, 987 (2006).
14. G. Girishkumar, M. Rettker, R. Underhile, D. Binz, K. Vinodgopal, P. McGinn, and P. Kamat, *Langmuir*, **21**, 8487 (2005).
15. Srivastava, O. N. Srivastava, S. Talapatra, R. Vajtai, and P. M. Ajayan, *Nat. Mater.*, **3**, 610 (2004).
16. W. J. Ma, L. Song, R. Yang, T. H. Zhang, Y. C. Zhao, L. F. Sun, Y. Ren, D. F. Liu, L. F. Liu, J. Shen, Z. X. Zhang, Y. J. Xiang, W. Y. Zhou, and S. S. Xie, *Nano Lett.*, **7**, 2307 (2007).
17. H. M. Kim, K. Kim, C. Y. Lee, J. Joo, S. J. Cho, H. S. Yoon, D. A. Pejakovic, J. W. Yoo, and A. J. Epstein, *J. Appl. Phys. Lett.*, **84**, 589 (2004).
18. B. Vigolo, P. Poulin, M. Lucas, P. Launois, and P. Bernier, *Appl. Phys. Lett.*, **81**, 1210 (2002).
19. Y. T. Shieh, G. L. Liu, H. H. Wu, and C. C. Lee, *Carbon*, **45**, 1880 (2007).
20. Y. Liu, L. Gao, and J. Sun, *J. Phys. Chem.,* **111**, 1223 (2007).
21. Y. J. Jeong, J. S. Kim, and G.-W. Lee, *Colloid Polym. Sci.*, **288**, 1 (2010).